

Research article

The Antimicrobial Activity of Silver Nanoparticles in Ag/Ag₂O Composites Synthesized by Oxygen Plasma Treatment of Silver Thin Films

Kamal Kayed^{1*} and Ghaytha Mansour²

¹Department of Physics, Faculty of Science, Damascus University, Damascus, Syria

²Department of Botany, Faculty of Science, Damascus University, Damascus, Syria

Received: 3 April 2021, Revised: 28 June 2021, Accepted: 9 August 2021

DOI: 10.55003/cast.2022.02.22.015

Abstract

Keywords

silver oxide;
individual silver;
nanoparticles;
thermal evaporation;
oxygen plasma afterglow;
Staphylococcus aureus;
inhibition zone tests

In this work, Ag/Ag₂O composites were synthesized by treating silver thin films manufactured by thermal evaporation method with oxygen plasma afterglow. In order to verify the antibacterial behavior of these composites, inhibition zone tests were realized for *Staphylococcus aureus*. The results showed that individual silver nanoparticles at concentrations that can be controlled by the stoichiometric ratios of the Ag/Ag₂O composites, were the main factor in the inhibition of bacteria. In addition, we found that the degree of degradation of individual silver nanoparticles absorption peaks represented a suitable criterion for determining the bacterial inhibition activity of the prepared silver oxide films. The results also showed that the sample treated at 1000 watts gave the highest rate of bacterial inhibition. This research includes an attempt to correlate the bacterial inhibition activity of silver oxide thin films with the structural and spectroscopic properties of these films.

1. Introduction

Silver nanoparticles (AgNPs) in AgNP/semiconductor composites cause unique modifications to the optical properties of the semiconductor. These modifications arise because of the formation of surface plasmon resonance (SPR) due to light-driven collective oscillations of conduction electrons in metallic AgNPs [1-8], which has the advantage of being both tunable and strong [8]. Therefore, the use of silver nanoparticles in Ag/Ag₂O composites is promising in many fields such as surface plasmon optics, catalysis, photonics, biosensing, photography, photo-catalytic technique, surface-enhanced Raman scattering, and in electronic devices such as sensors, solar cells, plasmon circuits and optical data storage medium [1-31].

*Corresponding author: Tel.: (+963) 988360356

E-mail: khmk2000@gmail.com

In the case of AgNP doping systems such as Ag/Ag₂O composites, any agglomeration in the plasmonic system of silver atoms due to the nature of the materials used may affect the measured luminescence and optical absorption spectra. Chiu [30] found that both the position and bandwidth of the plasmon bands in absorption spectra are strongly dependent on silver oxide (Ag₂O) grain size. Silver nanoparticle fluorescence emission spectra exhibit different characteristics when the laser excitation wavelength is varied [32]. In the same context, Zheng and Dickson [33] reported that only small Ag clusters synthesized by the photo-reduction technique could lead to intense fluorescence. In addition, they found that larger size of the nanoparticles synthesized by reduction with NaBH₄ was non-fluorescent. Maali *et al.* [34] found that in the case of silver nanoparticles prepared by spin-coating method, the coupling of silver atoms and silver oxide clusters determine the photo luminescent properties of the individual Ag particles.

In our previous work [21], we used oxygen plasma treatment of Ag thin films in the preparation of silver oxide (Ag₂O) thin films of high quality. The structural and optical properties of the prepared thin films were investigated. The results showed that exposing Ag thin films to oxygen plasma led to a monocrystalline structure of cubic-Ag₂O phase. It was also clearly shown that the plasma power has significant effects on the characteristics of all plasmon resonance peaks (position, spectral width and intensity). On the other hand, a slight degradation of the individual silver nanoparticles plasmon peaks was observed. It has been suggested that this decomposition occurs because of the mutual interaction between the individual silver nanoparticles located near Ag₂O grain shell and the larger Ag nanoparticles located in the neighboring grains. The results also showed that the degree of degradation was related to the grain size of silver oxide (Ag₂O).

One of common bacteria is *Staphylococcus aureus* which is a gram- positive, coagulase-positive, and golden color in culture [31]. It causes a wide range of clinical infections, and is resistant to β -lactam antibiotics. In this work, we attempt to establish relationships between the inhibitory activity of silver oxide films for *Staphylococcus aureus* and the structural and spectral properties of these films. Exploring and evaluating these equations will assist in determining appropriate parameters when manufacturing antibacterial systems.

2. Materials and Methods

2.1 Sample preparation

Pure silver metal thin films were deposited at room temperature onto thoroughly cleaned n-type Si (100) and glass substrates from a high-purity Ag target using a thermal evaporation system (JSM200). The substrate was placed above the target in the direction of the vapor flux. Table 1 contains the deposition process parameters.

Table 1. The deposition process parameters

Work pressure	Target current	Deposition time	Target purity	Deposition temperature	The film thickness
5x10 ⁻⁴ Pa	225 A	15 min	99.99%	25°C	316 nm

The oxidation process was done by placing each silver film in an evacuated pyrex tube and exposing it to a stream of oxygen plasma afterglow at a specific plasma power. The oxygen plasma stream was generated using a microwave SAIREM GMP 20 KEDS. More details about the plasma

generation system are available in previous work [35-37]. Table 2 contains the conditions of oxygen plasma exposure for each sample.

Table 2. The conditions of oxygen plasma exposure for each sample

Sample label	The film - discharge center distance	OPA power	plasma gas pressure	Processing time
a	0.25 m	250 W	300 Pa	30 min
b	0.25 m	500 W	300 Pa	30 min
c	0.25 m	750 W	300 Pa	30 min
d	0.25 m	1000 W	300 Pa	30 min
e	0.25 m	1250 W	300 Pa	30 min

The antibacterial activity of the prepared silver oxide thin films for *S. aureus* was evaluated by inhibition zone tests, which provides a qualitative measure of antibacterial activity based on the ratio between the growth inhibition zone area and the thin film area. A colony of *S. aureus* was taken from a fresh solid bacterium culture medium (Müller-Hinton agar) and was added to 20 ml of Müller-Hinton broth. Then, the resultant suspension was incubated overnight at 37°C and 120 rpm. A volume of 1 ml of 1×10^7 CFU ml⁻¹ cell suspension was added to 14 ml of Müller-Hinton agar at 45°C before pouring onto petri dish. Then, square samples of the different coatings were placed on the agar plates and incubated for 24 h at 37°C [31, 38].

2.2 Sample characterization

The crystallite structure of the prepared thin films was determined using a (Stoe StadiP) transmission X-ray diffractometer, employing a Cu K α_1 source ($\lambda = 1.54060 \text{ \AA}$).

3. Results and Discussion

X-ray diffraction measurements were carried out on the prepared silver oxide thin films. Figure 1 shows an example of the measured XRD spectra for sample (a), which was treated at 250 W. As seen in Figure 1, a strong X-ray diffraction peak is situated at $2\theta = 33.3$ degree, and is related to the (111) crystal plane of Ag₂O cubic phase (CSM Card No: 75-1532). We noticed that this peak is dominant in the XRD spectra of the samples b, c and d. Consequently, we concluded that the oxide layers in our samples were monocrystalline. More details about the characterization of the XRD measurement results are explained in our previous work [21]. Here, it is sufficient to include the values of the relative peak intensity (the oxide ratio) and the grain size of Ag₂O particles (Table 3) for each sample.

One common technique for evaluating the antibacterial activity of coatings is the halo formation method [31, 38], in which the appearance of a halo around a film placed on the surface of a bacterial colony is an indication of the formation of an inhibition zone of bacterial growth. In this work, we investigated the possibility of using samples prepared as described in Table 2 as antibacterial coatings. We adopted a criterion for measuring the effectiveness of inhibition, which is the ratio between the area of the effective inhibition zone (S') and the area of the film (S). Table 4 contains S, S' and S'/S of all the prepared thin films that were used in the bacterial inhibition tests. In addition, Figure 2 shows the region of plasma inhibition in the case of the sample treated at 250 W (sample a).

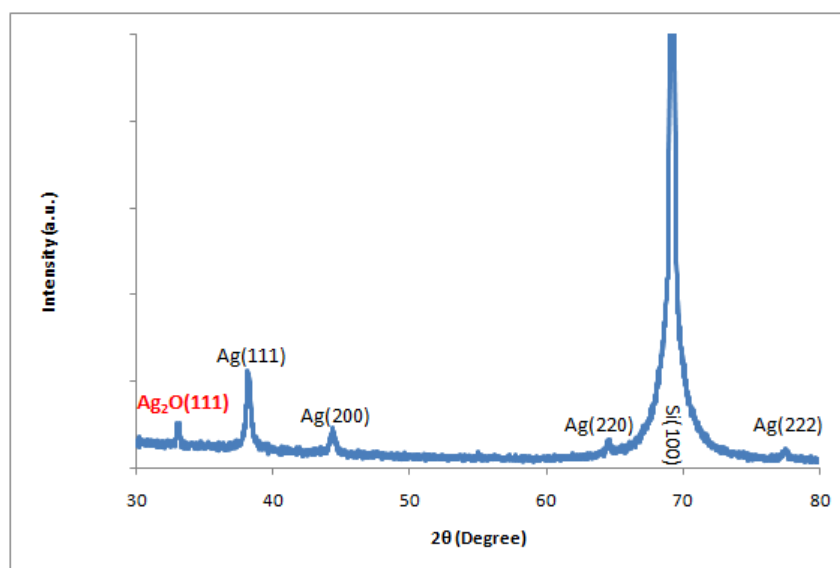


Figure 1. The XRD spectrum of the sample (a)

Table 3. The relative peak intensity and the grain size of Ag₂O particles for each sample

Sample	Ag ₂ O XRD peak intensity	The Ag ₂ O particles grain size
a	1.1831	5.347 (nm)
b	2.681	33.012 (nm)
c	3.642	34.941 (nm)
d	3.765	38.847 (nm)
e	1.805	7.412 (nm)

Table 4. The values of S, S' and S'/S of all the prepared thin films.

Sample label	S (cm ²)	S' (cm ²)	S'/S
a	3.90	6.00	1.538
b	4.68	6.16	1.316
c	2.08	3.08	1.481
d	2.60	4.20	1.615
e	5.20	0.00	0.000

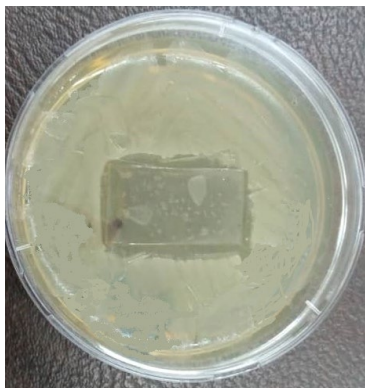


Figure 2. The region of plasma inhibition in the case of the sample treated at 250 W (sample a)

Figure 3 illustrates the ratio S'/S as a function of microwave plasma power. We noticed that there was no specific approach to the relationship between the S'/S ratio and the plasma power as the S'/S ratio value ranged between 1.32 and 1.62 for a, b, c and d samples. We noticed that using a plasma power of 1250 W led to a dramatic decrease in the S'/S ratio, which became equal to zero. This behavior can be explained by the low concentration of individual silver nanoparticles in this sample.

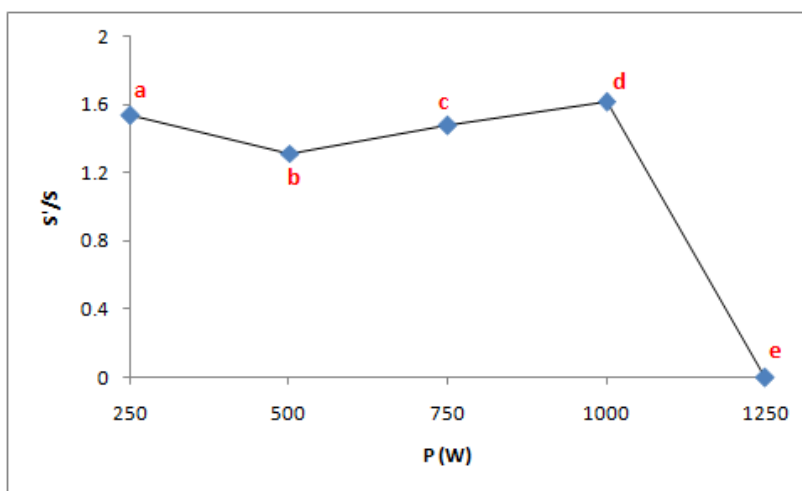


Figure 3. The ratio S'/S as a function of microwave plasma power

In the XRD spectrum, the oxide ratio in the film was proportional to the intensity of the Ag₂O peak. Figure 4 illustrates the ratio S'/S as a function of Ag₂O XRD peak intensity. We noticed that with the exception of sample (a), which had a metallic nature (due to its low oxygen content), the S'/S ratio increased with increasing silver oxide concentration. The same behavior can be seen in Figure 5, which represents the S'/S ratio as a function of the Ag₂O grain size. However, it seems that, the S'/S ratio appears to increase linearly with increasing grain size.

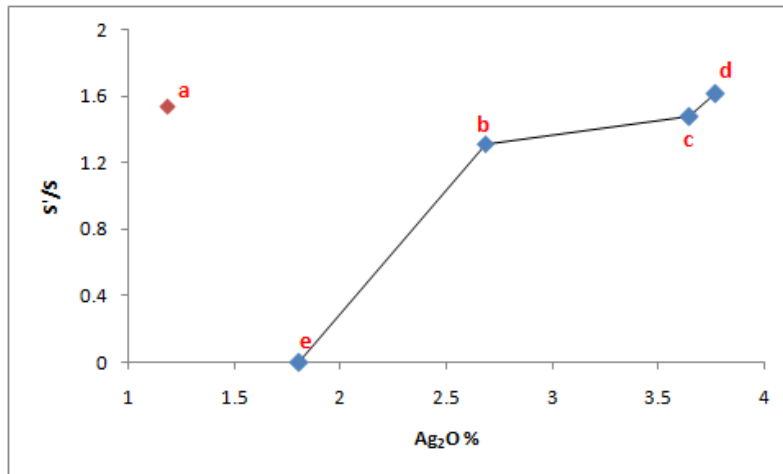


Figure 4. The ratio S'/S as a function of Ag₂O XRD peak intensity

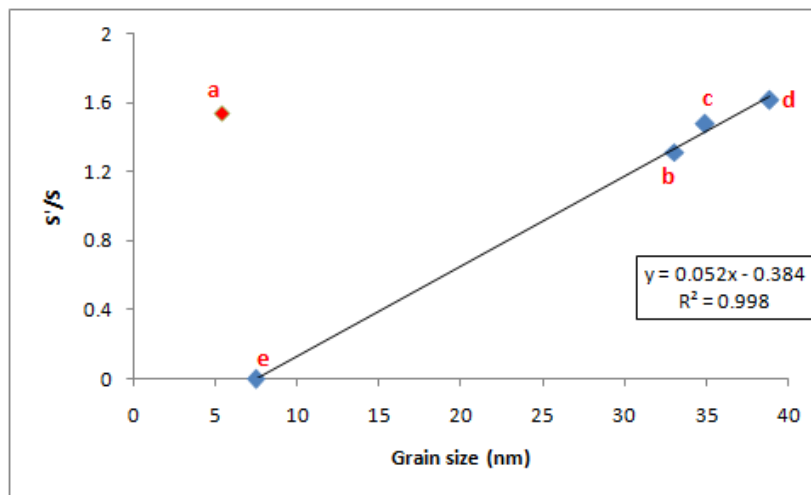


Figure 5. The ratio S'/S as a function of Ag₂O grain size

In Figures 5 and 6, point A (which represents a relatively high inhibition condition) is on the left side, which is the opposite side of the ratio S'/S decreasing trend. This gives the impression that both grain size and XRD Ag₂O peak intensity cannot be considered appropriate in all cases as measures of inhibition efficiency.

The measurement of the degradation of the individual silver nanoparticle plasmon peaks, which has been accurately described in our previous work [21], may be suitable for estimating the inhibitory activity of the bacterial growth. This degradation, which is related to the grain size of silver oxide, occurs due to the mutual interaction between the individual silver nanoparticles located near Ag₂O grain shell and the larger Ag nanoparticles located in the neighboring grains [21]. This degradation is measured using the ratio P_2/P_1 , which is equal to the ratio between the areas of the two peaks resulting from the degradation process [21]. Figure 6 shows the inhibition ratio S'/S as a function of the degradation ratio P_2/P_1 .

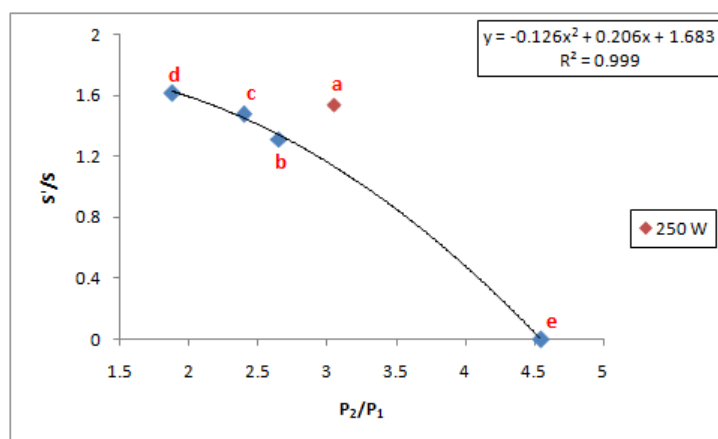


Figure 6. The ratio S'/S as a function of the ratio P_2/P_1

An interesting behavior can be observed in Figure 6 where the ratio S'/S decreases as the ratio P_2/P_1 increases, in a consistent manner. This result indicates that the inhibition activity is related to P_2/P_1 ratio. Accordingly, we conclude that individual silver nanoparticles are the main inhibitory centers. The more these atoms are isolated from the effects of neighboring silver configurations, the more effective the inhibition. On the other hand, it can be noted that the point (A) is located near the parabola formed from the rest of the experimental points. However, this point corresponds to a relatively high level of inhibition. It is close to the rest of the points, which makes it included in any criterion for the quality of inhibition that adopts a minimum value of the ratio P_2/P_1 .

What is particularly noteworthy here is that the sample (a) has an inhibitory effect, unlike sample (e), even though they have close values for grain size and silver oxide content. In fact, the explanation for this difference in the effectiveness of inhibition lies in the difference in the morphological structure of these two samples. While the higher concentration of silver metal leads to the attenuation of the plasmonic action in the sample (e), the porous structure and gaps within the structure reduce the effect of silver metal clusters in the case of the sample (a) [21]. In addition, the sample (a) contains a smaller percentage of larger Ag nanoparticles compared to the sample (e) [21]. These differences might lead to better interaction between the film surface and bacteria.

4. Conclusions

In this work, we tested the antibacterial activity of silver nanoparticles in Ag/Ag₂O composites synthesized by oxygen plasma treatment of silver thin films. We obtained unique results, which can be summarized as follows:

1. Individual silver nanoparticles are the main factor in the inhibition of bacteria.
2. With the exception of samples with a lower oxidation level, the inhibition efficacy is proportional to the Ag₂O grain.
3. The degree of degradation represents a suitable criterion for determining the bacterial inhibition activity of the prepared silver oxide films.
4. In the case of samples with low oxidation rates, the morphological structure plays an important role in determining ability to inhibit bacteria.

References

- [1] Sun, W., Hong, R., Liu, Q., Li, Z., Shi, J., Tao, C. and Zhang, D., 2019. SERS-active Ag–Al alloy nanoparticles with tunable surface plasmon resonance induced by laser ablation. *Optical Materials*, 96, 109298, <https://doi.org/10.1016/j.optmat.2019.109298>.
- [2] Ding, S.Y., Yi, J., Li, J.F., Ren, B., Wu, D.-Y., Panneerselvam, R. and Tian, Z.-Q., 2016. Nanostructure-based plasmon-enhanced Raman spectroscopy for surface analysis of materials. *Nature Reviews Materials*, 1(6), 16021-16036.
- [3] Chan, Y.F., Zhang, C.X., Wu, Z.L., Zhao, D.M., Wang, W., Xu, H.J. and Sun, X.M., 2013, Ag dendritic nanostructures as ultrastable substrates for surface-enhanced Raman scattering. *Applied Physics Letters*, 102, 183118, <https://doi.org/10.1063/1.4803937>.
- [4] Madhavi, V., Kondaiah, P. and Rao, G.M., 2018. Influence of silver nanoparticles on titanium oxide and nitrogen doped titanium oxide thin films for sun light photocatalysis. *Applied Surface Science*, 436, 708-719.
- [5] Low, J., Yu, J., Jaroniec, M., Wageh, S. and Al-Ghamdi, A.A., 2017. Heterojunction photocatalysts. *Advanced Materials*, 29, 1601694, <https://doi.org/10.1002/adma.201601694>.
- [6] Li, J., Fang, W., Yu, C., Zhou, W., Zhu, L. and Xie, Y., 2015. Ag-based semiconductor photocatalysts in environmental purification. *Applied Surface Science*, 358, 46-56.
- [7] Devi, L.G. and Kavitha, R., 2016. A review on plasmonic metal–TiO₂ composite for generation, trapping, storing and dynamic vectorial transfer of photogenerated electrons across the Schottky junction in a photocatalytic system. *Applied Surface Science*, 360, 601-622.
- [8] Maruno, S., 2019. Surface plasmon spectroscopy of thin composite films of Au nanoparticles and PEDOT:PSS conjugated polymer. *Organic Electronics*, 64, 154-157.
- [9] Detsri, E. and Popanyasak J., 2015. Fabrication of silver nanoparticles/polyaniline composite thin films using layer-by-layer self-assembly technique for ammonia sensing. *Colloids and Surfaces A: Physicochemical Engineering Aspects*, 467, 57-65.
- [10] Dubas, S.T. and Pimpan, V., 2008. Green synthesis of silver nanoparticles for ammonia sensing. *Talanta*, 76, 29-33.
- [11] Kayed, K. and Chiyah, B., 2020. The structural and optical properties of silver oxide thin films synthesized by thermal evaporation of silver with subsequent annealing. *Aerosol Science and Engineering*, 4(4), 271-276.
- [12] Li, Y., Leung, P., Yao, L., Song, Q.W. and Newton, E., 2006. Antimicrobial effect of surgical masks coated with nanoparticles. *Journal of Hospital Infection*, 62(1), 58-63.
- [13] Biswanath, M. and Moumita, M., 2009. Nonvolatile memory device based on Ag nanoparticle: characteristics improvement. *Applied Physics Letters*, 94, 233-236.
- [14] Chiyah, B. and Kayed, K., 2018. Effect of annealing temperature on the structural and optical properties of silver oxide thin films prepared by thermal evaporation with subsequent annealing. *International Journal of Nanoelectronics and Materials*, 11, 305-310.
- [15] Yang, G.-W. and Li, H., 2008. Sonochemical synthesis of highly monodispersed and size controllable Ag nanoparticles in ethanol solution. *Materials Letters*, 62(14), 2189-2191.
- [16] Li, S., Gao, B., Wang, Y., Jin, B., Yue, Q. and Wang, Z., 2019. Antibacterial thin film nanocomposite reverse osmosis membrane by doping silver phosphate loaded graphene oxide quantum dots in polyamide layer. *Desalination*, 464, 94-104.
- [17] Zhao, W.-B., Zhu, J.-J. and Chen, H.-Y., 2003. Photochemical synthesis of Au and Ag nanowires on a porous aluminum oxide template. *Journal of Crystal Growth*, 258, 176-180.
- [18] Dubas, S.T. and Pimpan, V., 2008. Humic acid assisted synthesis of silver nanoparticles and its application to herbicide detection. *Materials Letters*, 62, 2661-2663.
- [19] Dubas, S.T., 2007. *Preparation of Silver Nanoparticle Thin Films for Sensing Application*. Ph.D. Department of Material Science, Chulalongkorn University, Bangkok, Thailand.

- [20] Harinee, S., Muthukumar, K., Dahms, H.U., Koperuncholan, M., Vignesh, S., Banu, R.J., Ashok, M. and James, R.A., 2019. Biocompatible nanoparticles with enhanced photocatalytic and antimicrofouling potential. *International Biodeterioration & Biodegradation*, 145, 104790, <https://doi.org/10.1016/j.ibiod.2019.104790>.
- [21] Kayed, K., 2020. The optical properties of individual silver nanoparticles in Ag/Ag₂O composites synthesized by oxygen plasma treatment of silver thin films. *Plasmonics*, 15, 1439-1449.
- [22] Lakowicz, J., 2013. *Principles of Fluorescence Spectroscopy*. 3rd ed. New York: Springer.
- [23] Ling, L., Feng, Y., Li, H., Chen, Y., Wen, J., Zhu, J. and Bian, Z., 2019. Microwave induced surface enhanced pollutant adsorption and photocatalytic degradation on Ag/TiO₂. *Applied Surface Science*, 483, 772-778.
- [24] Mahapatra, S.S. and Karak, N., 2008. Silver nanoparticle in hyperbranched polyamine: synthesis, characterization and antibacterial activity. *Materials Chemistry and Physics*, 112, 1114-1119.
- [25] Wang, Y., 2006. A convenient route to polyvinyl pyrrolidone/silver nanocomposite by electrospinning. *Nanotechnology*, 17, 3304-3307.
- [26] Wadayama, H., Okabe, T., and Taniguchi, J., 2018. Fabrication of multilayered structure of silver nanorod arrays for plasmon memory. *Microelectronic Engineering*, 193, 47-53.
- [27] Li, M., Wang, Y., Xing, Y. and Zhong, J., 2020. P123-assisted preparation of Ag/Ag₂O with significantly enhanced photocatalytic performance. *Solid State Sciences* 99, 106062, <https://doi.org/10.1016/j.solidstatesciences.2019.106062>.
- [28] Uğur, Ş., Akaoglu, C. and Kucukkahveci, E., 2019. A study on film formation and fluorescence enhancement of PS latex/AgNPs composites depending on AgNPs content and annealing. *Colloids and Surfaces A*, 573, 40-56.
- [29] Ren, J. and Tilley R.D., 2007. Preparation, self-assembly, and mechanistic study of highly monodispersed nanocubes. *Journal of the American Chemical Society*, 129, 3287-3291.
- [30] Chiua, Y., 2003. Fabrication and nonlinear optical properties of nanoparticle silver oxide films. *Journal of Applied Physics*, 94, 1996-2001.
- [31] Hawser, S.P., Bouchillon, S.K., Hoban, D.J., Dowzicky, M. and Babinchak, T., 2011. Rising incidence of *Staphylococcus aureus* with reduced susceptibility to vancomycin and susceptibility to antibiotics: a global analysis 2004-2009. *International Journal of Antimicrobial Agents*, 37, 219-224.
- [32] Jian, Z., Xiang, Z. and Yongchang, W., 2005. Electrochemical synthesis and fluorescence spectrum properties of silver nanospheres. *Microelectronic Engineering*, 77, 58-62.
- [33] Zheng, J. and Dickson, R.M., 2002. Individual water-soluble dendrimer-encapsulated silver nanodot fluorescence. *Journal of the American Chemical Society*, 124, 13982-13983.
- [34] Maalia, A., Cardinal, T. and Treguer-Delapierre, M., 2003. Intrinsic putrescence from individual silver nanoparticles. *Physica E*, 17, 559-560.
- [35] Alkhawwam, A., Abdallaha, B., Kayed, K. and Alshoufi, K., 2011. Effect of nitrogen plasma afterglow on amorphous carbon nitride thin films deposited by laser ablation. *Acta Physica Polonica*, 120, 545-551.
- [36] Kayed, K., 2010. *Synthesis and Properties of Carbon Nitride and Boron Nitride Thin Films Prepared by Different Techniques*. PhD. Damascus University Syria, Damascus.
- [37] Kayed, K., 2018. Effect of nitrogen plasma afterglow on the (1000-1800) cm⁻¹ band in FTIR spectra of amorphous carbon nitride thin films. *Spectrochimica Acta Part A: Molecular and Biomolecular Spectroscopy*, 190, 253-258.
- [38] Rebelo, R., Manninen, N.K., Fialho, L., Henriques, M. and Carvalho, S., 2016. Morphology and oxygen incorporation effect on antimicrobial activity of silver thin films. *Applied Surface Science*, 371, 1-8.